



STATIONARY LOCALIZED SOLUTIONS IN THE SUBCRITICAL COMPLEX GINZBURG–LANDAU EQUATION

O. DESCALZI

*Facultad de Ingeniería, Universidad de los Andes,
Av. San Carlos de Apoquindo 2200, Santiago-Chile*

M. ARGENTINA and E. TIRAPEGUI

*Departamento de Física, F.C.F.M. Universidad de Chile,
Casilla 487-3, Santiago-Chile*

*Centro de Física No Lineal y Sistemas Complejos de Santiago,
Casilla 27122, Santiago-Chile*

Received February 23, 2002; Revised March 18, 2002

It is shown that pulses in the complete quintic one-dimensional Ginzburg–Landau equation with complex coefficients appear through a saddle-node bifurcation which is determined analytically through a suitable approximation of the explicit form of the pulses. The results are in excellent agreement with direct numerical simulations.

Keywords: Ginzburg–Landau equation; saddle-node bifurcation; localized structures.

1. Introduction

The discovery of confined traveling waves in convection in binary fluids [Heinrichs *et al.*, 1987; Kolodner *et al.*, 1987; Kolodner *et al.*, 1988; Niemela *et al.*, 1990; Moses *et al.*, 1987] has been a motivation for theoretical work on localized solutions of amplitude equations [Afanasjev *et al.*, 1996; Akhmediev *et al.*, 1996; Deissler & Brand, 1990, 1994, 1995; Fauve & Thual, 1990; Hakim & Pomeau, 1991; Malomed & Nepomnyashchy, 1990; Marcq *et al.*, 1994; Soto-Crespo *et al.*, 1997; Thual & Fauve, 1988; van Saarloos & Hohenberg, 1990; van Saarloos & Hohenberg, 1992]. Nevertheless most of this work has been devoted to numerical analysis. The aim of this article is to give an analytical approach to the study of stationary localized solutions in the subcritical complex Ginzburg–Landau equation.

When the equilibrium state of an extended system loses stability through a subcritical Hopf

bifurcation it is described near threshold by its normal form [Elphick *et al.*, 1987] which is the quintic Ginzburg–Landau equation with complex coefficients for a complex amplitude $A(x, t)$:

$$\begin{aligned} \partial_t A = & \tilde{\mu}A + (\beta_r + i\beta_i)|A|^2 A + (\gamma_r + i\gamma_i)|A|^4 A \\ & + (D_r + iD_i)\partial_{xx} A. \end{aligned} \quad (1)$$

2. Stationary Localized Solutions

We look for localized solutions making the Ansatz

$$A = R_0(x) \exp\{i(\Omega t + \theta_0(x))\}, \quad (2)$$

where Ω is an unknown parameter. Replacing (2) in (1) we obtain

$$\begin{aligned} 0 = & \tilde{\mu}R_0 + \beta_r R_0^3 + \gamma_r R_0^5 + D_r(R_{0xx} - R_0\theta_{0x}^2) \\ & - D_i(2R_{0x}\theta_{0x} + R_0\theta_{0xx}) \end{aligned} \quad (3)$$

and

$$\Omega R_0 = \beta_i R_0^3 + \gamma_i R_0^5 + D_r(2R_{0x}\theta_{0x} + R_0\theta_{0xx}) + D_i(R_{0xx} - R_0\theta_{0x}^2), \tag{4}$$

where the indices x stand for derivatives with respect to the variable x .

After some simple algebra these equations can be written in the form

$$0 = \mu_+ R_0 + \beta_+ R_0^3 + \gamma_+ R_0^5 + R_{0xx} - R_0\theta_{0x}^2. \tag{5}$$

and

$$\mu_- R_0 = \beta_- R_0^3 + \gamma_- R_0^5 + 2R_{0x}\theta_{0x} + R_0\theta_{0xx}, \tag{6}$$

where

$$\mu_+ = \frac{D_r\tilde{\mu} - D_i\Omega}{|D|^2}; \quad \beta_+ = \frac{D_r\beta_r + D_i\beta_i}{|D|^2}; \tag{7}$$

$$\gamma_+ = \frac{D_r\gamma_r + D_i\gamma_i}{|D|^2}$$

$$\mu_- = \frac{D_i\tilde{\mu} + D_r\Omega}{|D|^2}; \quad \beta_- = \frac{D_r\beta_i - D_i\beta_r}{|D|^2}; \tag{8}$$

$$\gamma_- = \frac{D_r\gamma_i - D_i\gamma_r}{|D|^2}$$

and $|D|^2 = D_r^2 + D_i^2$. We remark that (5) and (6) have the same form as the equations obtained with a similar Ansatz from (1) when dispersive effects are neglected, i.e. $D_i = 0$. We have studied these equations in [Descalzi *et al.*, 2002] and we can see that the only effect of putting $D_i \neq 0$ is to renormalize the coefficients which take here the values given by (7) and (8). In order to solve approximately (5) and (6) we use then the same strategy which consists in dividing the x axis into a core region \mathcal{R}_1 and a region \mathcal{R}_2 outside the core of the pulse. In \mathcal{R}_1 we approximate the functions $R_0(x)$ and θ_{0x} by their first terms in a Taylor expansion writing

$$R_0(x) = R_m - \varepsilon x^2, \quad \theta_{0x} = -\alpha x, \tag{9}$$

where $(R_m, \varepsilon, \alpha)$ are unknown quantities. Replacing (9) in (5) and (6) we obtain ε and α in terms of (Ω, R_m) and the parameters of (1) [see (7) and (8)]. One has

$$\varepsilon = \frac{1}{2}(\mu_+ R_m + \beta_+ R_m^3 + \gamma_+ R_m^5) \tag{10}$$

$$\alpha = \beta_- R_m^2 + \gamma_- R_m^4 - \mu_- . \tag{11}$$

We see in (9) that in the core \mathcal{R}_1 we are approximating the modulus of the pulse by a parabola with a maximum R_m and $\theta_{0x} = d\theta_0/dx$ by a straight line with slope α . Outside the core, in the region \mathcal{R}_2 , we approximate the phase $\theta_{0x}(x)$ putting $\theta_{0x}(x) = p$ for $x < 0$ and $\theta_{0x}(x) = -p$ for $x > 0$. Assuming that $R_0(x)$ vanishes exponentially for $|x| \rightarrow \infty$ we obtain asymptotically for $x \rightarrow \infty$ that Eqs. (5) and (6) reduce to

$$-2R_{0x}p = \mu_- R_0, \quad R_{0xx} = R_0(-\mu_+ + p^2). \tag{12}$$

The second equation gives

$$R_0(x) = C \exp\{-\sqrt{-\mu_+ + p^2}x\},$$

then $R_{0x}/R_0 = -\sqrt{-\mu_+ + p^2}$ for big x and from the first equation we obtain

$$\mu_- = 2p\sqrt{-\mu_+ + p^2}. \tag{13}$$

From this expression we can obtain Ω in terms of p :

$$\Omega = \frac{1}{D_r^2}(-D_i(\tilde{\mu}D_r - 2p^2|D|^2) + 2p|D|^2\sqrt{-\tilde{\mu}D_r + p^2|D|^2}). \tag{14}$$

In fact we can integrate explicitly Eq. (5) in \mathcal{R}_2 putting $\theta_{0x}^2 = p^2$. The result is

$$R_0(x) = \frac{2b^{\frac{1}{4}} \exp\{\sqrt{-\mu_+ + p^2}(|x| + x_0)\}}{\sqrt{\left(\exp\{2\sqrt{-\mu_+ + p^2}(|x| + x_0)\} + \frac{a}{\sqrt{b}}\right)^2 - 4}}, \tag{15}$$

where $a = -3\beta_+/2\gamma_+$, $b = -3(-\mu_+ + p^2)/\gamma_+$ and x_0 is a constant to be determined. We remark that at this point we know the parameters $(\varepsilon, \alpha, \Omega)$ as functions of (R_m, p) through Eqs. (10), (11) and (14). The next step is to match $R_0(x)$ in regions \mathcal{R}_1 and \mathcal{R}_2 . This is done at the point $(x_*, r_c) \equiv (-(p/\alpha), R_m - \varepsilon x_*^2)$ which has an obvious geometrical interpretation: r_c is the value of $R_0(x)$ at the matching point $x_* = -(p/\alpha)$ which is such that

$$\begin{aligned} \theta_{0x} &= p \quad (x < x_*), \quad \theta_{0x} = -p \quad (x > -x_*); \\ \theta_{0x} &= -\alpha x, \quad x \in \left[-\frac{p}{\alpha}, \frac{p}{\alpha}\right]. \end{aligned} \tag{16}$$

Using (15) we obtain

$$u_*^2 = -\left(\frac{a}{\sqrt{b}} - \frac{2\sqrt{b}}{r_c^2}\right) + \sqrt{\left(\frac{a}{\sqrt{b}} - \frac{2\sqrt{b}}{r_c^2}\right)^2 - \left(\frac{a^2}{b} - 4\right)}, \tag{17}$$

where $u_* = \exp\{-\sqrt{-\mu_+ + p^2}(x_* - x_0)\}$. Then:

$$x_0 = x_* + \frac{\ln u_*}{\sqrt{-\mu_+ + p^2}}. \quad (18)$$

After using the expressions (10) and (11) for ε and α , the last two Eqs. (17) and (18) determine x_0 in terms of (R_m, p) . We match now the derivative $dR_0(x)/dx$ at the same point x_* .

From $R_0(x)$ outside the core in region \mathcal{R}_2 [see (15)] we obtain

$$\begin{aligned} & \left(\frac{dR_0(x)}{dx}\right)_{x=x_*-0} \\ &= -\sqrt{-\mu_+ + p^2} \left(r_c - \frac{r_c^3 \left(u_*^2 + \frac{a}{\sqrt{b}}\right)}{2\sqrt{b}} \right). \end{aligned} \quad (19)$$

Inside the core the derivative is calculated from (9) and one has

$$\left(\frac{dR_0(x)}{dx}\right)_{x=x_*+0} = -2\varepsilon x_*. \quad (20)$$

Equalizing (19) and (20) we get the relation

$$f(R_m, p) \equiv \sqrt{-\frac{\gamma_+}{3}} r_c \sqrt{r_c^4 - ar_c^2 + b} + 2\varepsilon x_* = 0. \quad (21)$$

$$\begin{aligned} \int_{-\infty}^0 R_0^6 dx &= \frac{\sqrt{-\frac{3}{\gamma_+}}}{16(-4b + (a + \sqrt{b}u_*^2)^2)^2} \left(-12a\sqrt{b}(a^2 - 4b)^2 - 4bu_*^2(a^2 - 4b)(9a^2 + 4b) - 12a(3a^2 - 4b)b^{\frac{3}{2}}u_*^4 \right. \\ &\quad \left. + 4b^2(-3a^2 + 4b)u_*^6 + (3a^2 - 4b)(-4b + (a + \sqrt{b}u_*^2)^2)^2 \ln \left| \frac{a + \sqrt{b}(u_*^2 + 2)}{a + \sqrt{b}(u_*^2 - 2)} \right| \right) \\ &\quad - R_m^6 x_* + 2R_m^5 \varepsilon x_*^3. \end{aligned} \quad (25)$$

3. Saddle-Node Bifurcation

In order to see that the appearance of pulses in the complex Ginzburg–Landau equation is related to a saddle-node bifurcation we shall study in the two dimensional space (R_m, p) the intersections of the two curves $f(R_m, p) = 0$ and $g(R_m, p) = 0$ [see Eqs. (21) and (22)]. We scale first time, space and the amplitude A in (1) putting $t = \sigma t'$, $x = \lambda x'$, $A(x, t) = \nu A'(x', t')$. In our case $\beta_r > 0$, $D_r > 0$, $\gamma_r < 0$ (we want coexistence of homogeneous

A second relation between R_m and p is obtained multiplying Eq. (6) by $R_0(x)$ and integrating on the real axis. Since $R_0(x)$ is a symmetric function the result can be written as

$$\begin{aligned} g(R_m, p) &\equiv \mu_- - \beta_- \frac{\int_{-\infty}^0 R_0^4 dx}{\int_{-\infty}^0 R_0^2 dx} - \gamma_- \frac{\int_{-\infty}^0 R_0^6 dx}{\int_{-\infty}^0 R_0^2 dx} \\ &= 0. \end{aligned} \quad (22)$$

All the integrals in (22) can be calculated and one obtains

$$\begin{aligned} \int_{-\infty}^0 R_0^2 dx &= \frac{1}{2} \sqrt{-\frac{3}{\gamma_+}} \ln \left| \frac{a + \sqrt{b}(u_*^2 + 2)}{a + \sqrt{b}(u_*^2 - 2)} \right| \\ &\quad - R_m^2 x_* + \frac{2}{3} R_m \varepsilon x_*^3. \end{aligned} \quad (23)$$

$$\begin{aligned} \int_{-\infty}^0 R_0^4 dx &= -\sqrt{-\frac{3}{\gamma_+}} \frac{(a^2 - 4b)\sqrt{b} + abu_*^2}{(-4b + (a + \sqrt{b}u_*^2)^2)} \\ &\quad + \frac{a}{4} \sqrt{-\frac{3}{\gamma_+}} \ln \left| \frac{a + \sqrt{b}(u_*^2 + 2)}{a + \sqrt{b}(u_*^2 - 2)} \right| \\ &\quad - R_m^4 x_* + \frac{4}{3} R_m^3 \varepsilon x_*^3. \end{aligned} \quad (24)$$

attractors), and choosing $\nu = \sqrt{\beta_r/|\gamma_r|}$, $\sigma = |\gamma_r|/\beta_r^2$, $\lambda = \sqrt{D_r|\gamma_r|}/\beta_r$, Eq. (1) becomes (omitting the primes)

$$\begin{aligned} \partial_t A &= \mu A + (1 + i\beta)|A|^2 A \\ &\quad - (1 + i\gamma)|A|^4 A + (1 + i\alpha)\partial_{xx} A, \end{aligned} \quad (26)$$

with $\mu = \tilde{\mu}(|\gamma_r|/\beta_r^2)$, $\alpha = D_i/D_r$, $\beta = \beta_i/\beta_r$, $\gamma = \gamma_i/\gamma_r$. We fix now $\beta = 0.2$, $\gamma = -0.15$, $\alpha = -0.1$, and study Eq. (26) varying μ . For

$\mu = \mu_{c1} = -0.16776$ the curves $f(R_m, p) = 0$ (continuous line) and $g(R_m, p) = 0$ (dashed line) cut tangentially giving origin to a saddle-node bifurcation [Fig. 1(a)]. Above μ_{c1} these curves cut at two points

giving origin to a pair of pulses [Fig. 1(b)]. One of them stable and the other one unstable.

Under $\mu = \mu_{c2} = -0.118$ the intersection of the curves $f(R_m, p) = 0$ and $g(R_m, p) = 0$ still predicts

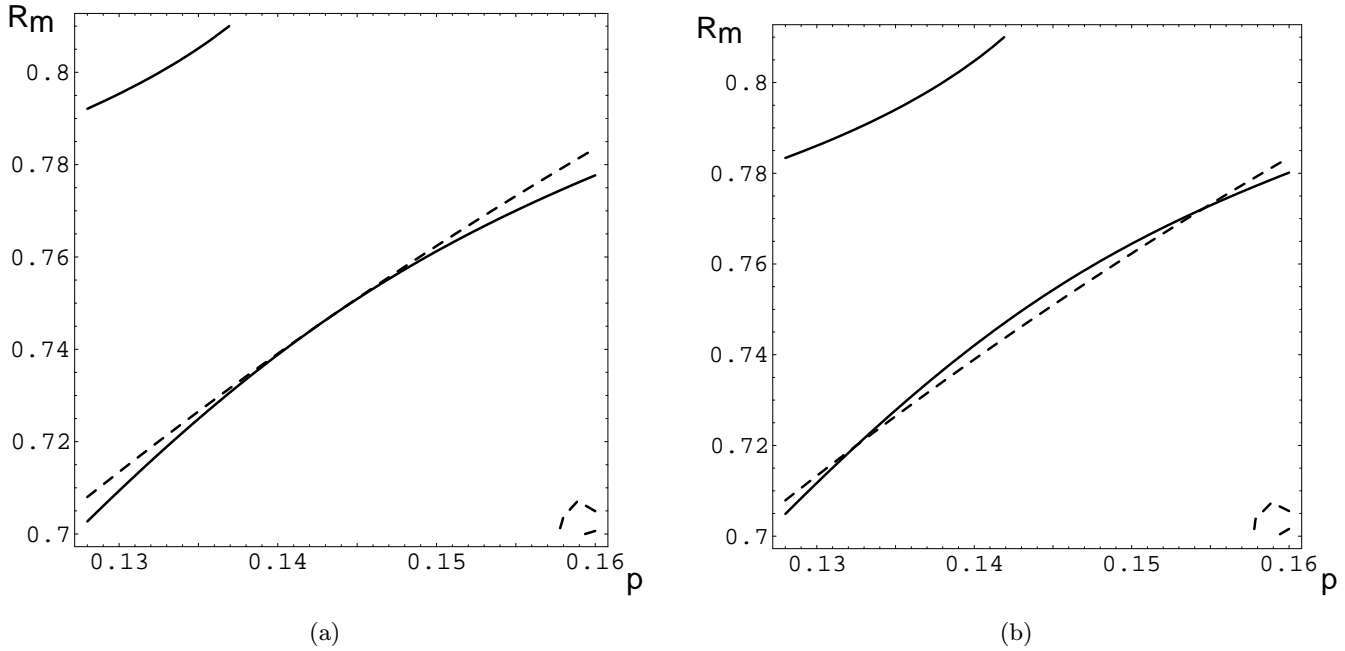


Fig. 1. (a) For $\mu = \mu_{c1} = -0.16776$ the curves $f = g = 0$ cut tangentially. (b) For $\mu = -0.167 > \mu_{c1}$ the curves $f = g = 0$ cut at two points.

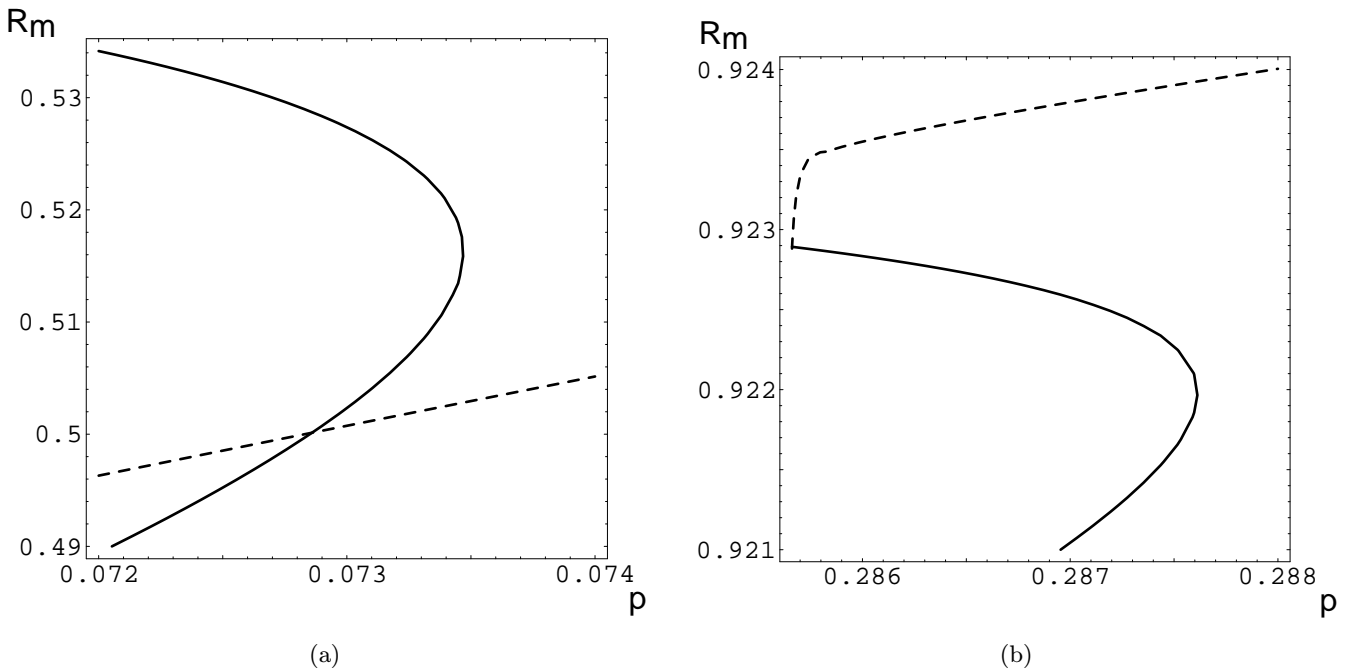


Fig. 2. (a) For $\mu = \mu_{c2} = -0.118$ the intersection between the curves $f = g = 0$ predicts an unstable pulse. (b) The intersection predicting a stable pulse.

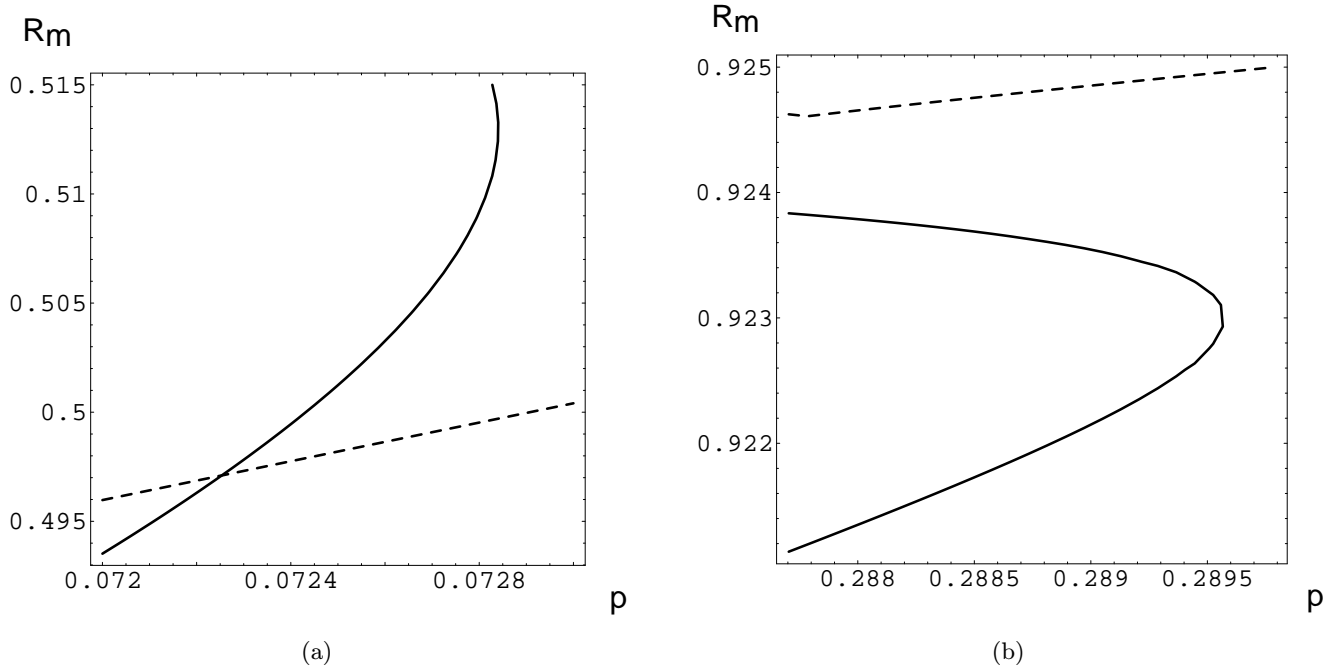


Fig. 3. (a) For $\mu = -0.117 > \mu_{c2}$ the intersection between the curves $f = g = 0$ predicts an unstable pulse. (b) The curves $f = g = 0$ do not intersect forbidding the existence of a stable pulse.

the existence of two pulses. In Fig. 2(a) the intersection predicts one unstable pulse and in Fig. 2(b) one stable pulse.

Above $\mu = \mu_{c2} = -0.118$ Fig. 3 shows that there still exist an intersection between the curves $f = g = 0$ predicting an unstable pulse [Fig. 3(a)], but one does not get an intersection corresponding to the stable pulse [Fig. 3(b)].

In Fig. 4 we see explicitly the character of the saddle-node bifurcation. We computed Ω as a function of μ using the expression given by (14) (thick continuous line stands for stable pulses and thick dashed line stands for unstable pulses) and we compare with the curve obtained using the bifurcation software auto 2000 [Doedel *et al.*, 1991] (thin continuous line). The software shows that near $\mu = -0.168$ and $\mu = -0.11$ the system undergoes a saddle-node bifurcation. Both critical values of μ are in very well agreement with the theoretical predicted values for μ_{c1} and μ_{c2} . Moreover both curves show that the branch corresponding to the unstable pulses persists up to $\mu = 0$.

A direct numerical simulation of Eq. (26), with parameters $\mu = -0.13$, $\beta = 0.2$, $\gamma = -0.15$, $\alpha = -0.1$ has been carried out. Owing to the fact that the curves $f(R_m, p) = 0$ and $g(R_m, p) = 0$ cut at two points, namely, $p = 0.08072$; $R_m = 0.537686$ and $p = 0.262542$; $R_m = 0.90928$, we predict two

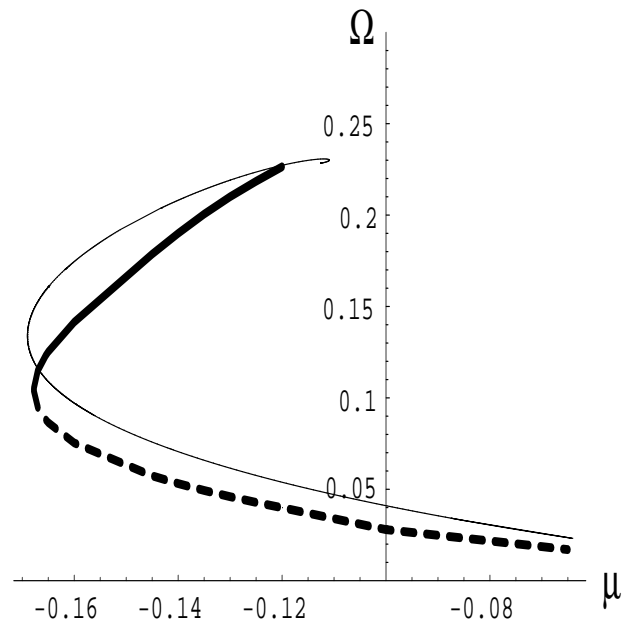


Fig. 4. Bifurcation diagram for pulses. The theoretical bifurcation curve is drawn with thick line (continuous line stands for stable pulses and dashed line stands for unstable pulses). The bifurcation curve computed with software auto 2000 is drawn with thin continuous line.

pulses. In Fig. 5(a) we show the shapes of the pulses obtained with our analytical approach. The continuous line corresponds to the stable pulse and the dashed line to the unstable one. The pulse

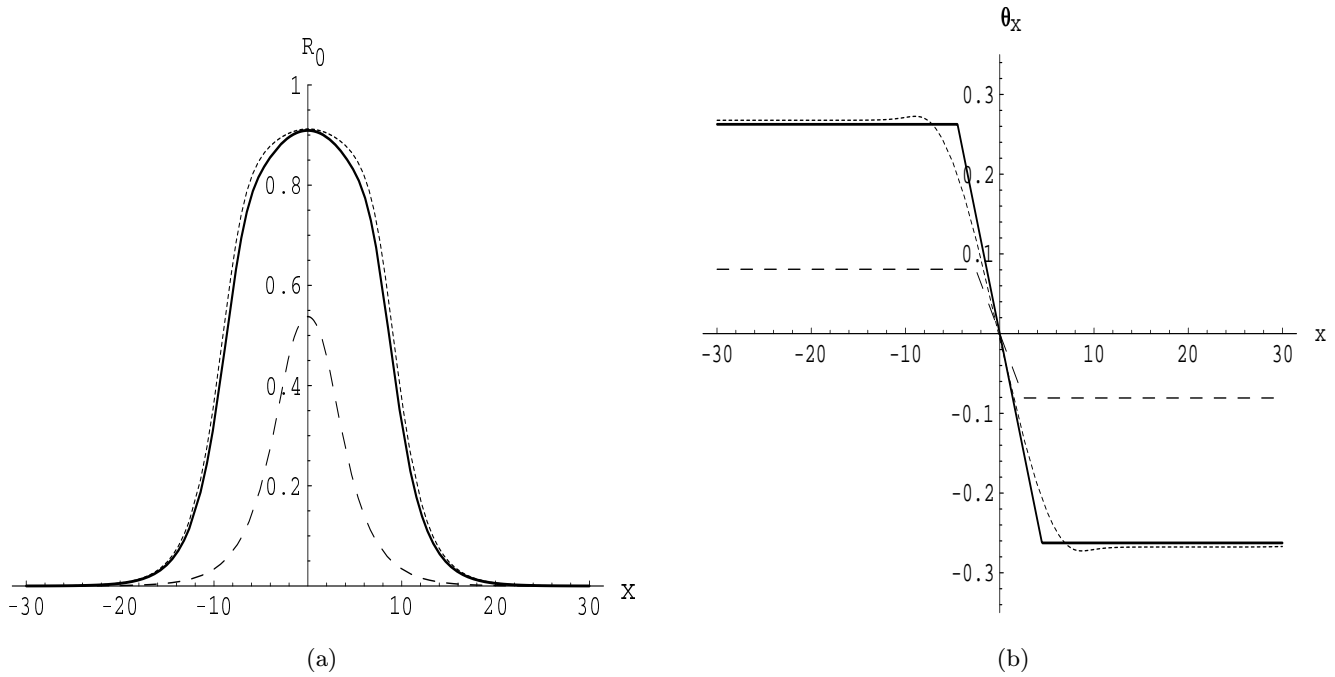


Fig. 5. (a) Shape of the stable and unstable pulses predicted by the analytical approach (continuous and dashed lines). The numerical result is represented by punctured line. (b) The gradient of the phase.

obtained from the direct numerical simulation is drawn with the punctured line. The values of R_m and the asymptotical value of the phase gradient agree within 1% of our analytical approach. In Fig. 5(b) we show the gradient of the phase for the three above mentioned cases.

Acknowledgments

E. Tirapegui and O. Descalzi wish to thank Fondo de Ayuda a la Investigación of the U. de los Andes (Project ICIV-001-02) and FONDECYT (P. 1020374). M. Argentina acknowledges the support from FONDECYT (P. 3000017). We would like to thank Dr. Marcel Clerc (Universidad de Chile) and Prof. Helmut Brand (Universitaet Bayreuth, Germany) for many useful discussions. The numerical simulations have been performed using the software developed in the Institute Nonlinéaire de Nice, France. We are indebted to Prof. P. Coulet (Nice) for allowing us to use this software.

References

- Afanasjev, V. V., Akhmediev, N. & Soto-Crespo, J. M. [1996] "Three forms of localized solutions of the quintic complex Ginzburg–Landau equation," *Phys. Rev.* **E53**, 1931–1939.
- Akhmediev, N., Afanasjev, V. V. & Soto-Crespo, J. M. [1996] "Singularities and special soliton solutions of the cubic-quintic complex Ginzburg–Landau equation," *Phys. Rev.* **E53**, 1190–1201.
- Deissler, R. J. & Brand, H. R. [1990] "The effect of nonlinear gradient terms on localized states near a weakly inverted bifurcation," *Phys. Lett.* **A146**, 252–255.
- Deissler, R. J. & Brand, H. R. [1994] "Periodic, quasiperiodic, and chaotic localized solutions of the quintic complex Ginzburg–Landau equation," *Phys. Rev. Lett.* **72**, 478–481.
- Deissler, R. J. & Brand, H. R. [1995] "Two-dimensional localized solutions for the subcritical bifurcations in systems with broken rotational symmetry," *Phys. Rev.* **E51**, R852–R855.
- Descalzi, O., Argentina, M. & Tirapegui, E. [2002] "Saddle-node bifurcation: An appearance mechanism of pulses in the subcritical complex Ginzburg–Landau equation," submitted to *Phys. Rev. E*.
- Doedel, E. J., Keller, H. B. & Kernévez, J. P. [1991] "Numerical analysis and control of bifurcation problems, Part II: Bifurcation in infinite dimensions," *Int. J. Bifurcation and Chaos* **1**(4), 745–772.
- Elphick, E., Tirapegui, E., Brachet, M. E., Coulet, P. & Iooss, G. [1987] "A simple global characterization for normal forms of singular vector field," *Physica* **D29**, 95–127.
- Fauve, S. & Thual, O. [1990] "Solitary waves generated by subcritical instabilities in dissipative systems," *Phys. Rev. Lett.* **64**, 282–284.

- Hakim, V. & Pomeau, Y. [1991] “On stable localized structures and subcritical instabilities,” *Eur. J. Mech. B/Fluids. Suppl.* **10**, 137–143.
- Heinrichs, R., Ahlers, G. & Cannell, D. S. [1987] “Traveling waves and spatial variation in the convection of a binary mixture,” *Phys. Rev.* **A35**, 2761–2764.
- Kolodner, P., Surko, C. M., Passner, A. & Williams, H. L. [1987] “Pulses of oscillatory convection,” *Phys. Rev.* **A36**, 2499–2502.
- Kolodner, P., Bensimon, D. & Surko, C. M. [1988] “Traveling-wave convection in an annulus,” *Phys. Rev. Lett.* **60**, 1723–1726.
- Malomed, B. A. & Nepomnyashchy, A. A. [1990] “Kinks and solitons in the generalized Ginzburg–Landau equation,” *Phys. Rev.* **A42**, 6009–6014.
- Marcq, P., Chaté, H. & Conte, R. [1994] “Exact solutions of the one-dimensional quintic complex Ginzburg–Landau equation,” *Physica* **D73**, 305–317.
- Moses, E., Fineberg, J. & Steinberg, V. [1987] “Multistability and confined traveling-wave patterns in a convecting binary mixture,” *Phys. Rev.* **A35**, 2757–2760.
- Niemela, J. J., Ahlers, G. & Cannell, D. S. [1990] “Localized traveling-wave states in binary-fluid convection,” *Phys. Rev. Lett.* **64**, 1365–1368.
- Soto-Crespo, J. M., Akhmediev, N., Afanasjev, V. V. & Wabnitz, S. [1997] “Pulse solutions of the cubic-quintic complex Ginzburg–Landau equation in the case of normal dispersion,” *Phys. Rev.* **E55**, 4783–4796.
- Thual, O. & Fauve, S. [1988] “Localized structures generated by subcritical instabilities,” *J. Phys. France* **49**, 1829–1833.
- van Saarloos, W. & Hohenberg, P. C. [1990] “Pulses and fronts in the complex Ginzburg–Landau equation near a subcritical bifurcation,” *Phys. Rev. Lett.* **64**, 749–752.
- van Saarloos, W. & Hohenberg, P. C. [1992] “Fronts, pulses, sources and sinks in generalized complex Ginzburg–Landau equations,” *Physica* **D56**, 303–367.